

Detection of edge magnetic state by a ballistic bend resistance measurement

Takahiro Matsunaga, Kohsuke Furukawa, Yuhsuke Kanda, Masahiro Hara, Tatsuya Nomura, and Takashi Kimura

Citation: [Applied Physics Letters](#) **102**, 252405 (2013); doi: 10.1063/1.4812729

View online: <http://dx.doi.org/10.1063/1.4812729>

View Table of Contents: <http://scitation.aip.org/content/aip/journal/apl/102/25?ver=pdfcov>

Published by the [AIP Publishing](#)

Articles you may be interested in

[Quantitative investigation of magnetic domains with in-plane and out-of-plane easy axes in GaMnAs films by Hall effect](#)

[J. Appl. Phys.](#) **113**, 17C706 (2013); 10.1063/1.4794283

[Detection of charge states in nanowire quantum dots using a quantum point contact](#)

[Appl. Phys. Lett.](#) **90**, 172112 (2007); 10.1063/1.2732829

[Switching of magnetic domains in Permalloy microstructures using two-dimensional electron gas](#)

[Appl. Phys. Lett.](#) **89**, 182513 (2006); 10.1063/1.2378488

[Perpendicular magnetization reversal, magnetic anisotropy, multistep spin switching, and domain nucleation and expansion in Ga_{1-x}Mn_xAs films](#)

[J. Appl. Phys.](#) **98**, 063904 (2005); 10.1063/1.2043233

[Control of magnetization states in microstructured permalloy rings](#)

[Appl. Phys. Lett.](#) **84**, 939 (2004); 10.1063/1.1646223

The advertisement features a blue background with a glowing light effect and a molecular structure. On the left, there is a small image of the 'AIP Applied Physics Reviews' journal cover, which shows a 3D diagram of a layered structure. The main text 'NEW Special Topic Sections' is in large white font. Below it, 'NOW ONLINE' is in yellow, followed by 'Lithium Niobate Properties and Applications: Reviews of Emerging Trends' in white. The AIP Applied Physics Reviews logo is in the bottom right corner.

NEW Special Topic Sections

NOW ONLINE
Lithium Niobate Properties and Applications:
Reviews of Emerging Trends

AIP Applied Physics Reviews

Detection of edge magnetic state by a ballistic bend resistance measurement

Takahiro Matsunaga,¹ Kohsuke Furukawa,¹ Yuhsuke Kanda,¹ Masahiro Hara,^{1,a)}
 Tatsuya Nomura,² and Takashi Kimura²

¹Graduate School of Science and Technology, Kumamoto University, 2-39-1 Kurokami,
 Kumamoto 860-8555, Japan

²Advanced Electronics Research Division, INAMORI Frontier Research Center, Kyushu University,
 744 Motoooka, Fukuoka 819-0395, Japan

(Received 15 March 2013; accepted 16 June 2013; published online 27 June 2013)

We have investigated a magnetization process of a permalloy nanowire by using a ballistic micro-Hall sensor consisting of GaAs/AlGaAs two-dimensional electron gas. Although a conventional bi-stable hysteresis loop with a rectangular shape was observed in the Hall resistance measurement, unexpected extra resistance changes were observed in a bend resistance measurement. These unconventional features are quantitatively explained by the magnetic transitions among the meta-stable edge-domain structures in the ferromagnetic wire. The geometrical dependence of these resistance changes and their application possibility for the multiple-valued memory were also discussed. © 2013 AIP Publishing LLC. [<http://dx.doi.org/10.1063/1.4812729>]

Magnetic field sensors are widely utilized in commercial electrical and biomedical devices as well as in the fundamental analysis of the functional magnetic materials.¹ Various types of the magnetic sensors have been developed and still continue to grow with improving the performance and the cost reduction. Fluxgate sensor using a magnetic core is known to provide high sensitivity with a reliable room-temperature operation. However, complexities of the device structures make it difficult to reduce the device dimension. In addition, it is not suitable to detect the spatially non-uniform magnetic field. Superconducting quantum interference device (SQUID) sensor yields the highest field sensitivity less than pico Tesla. However, its operation is limited to low temperature because of the necessity of the superconductivity, leading to high running cost and large system size. The use of spin-dependent transports such as giant and tunnel magneto-resistances (MRs) enables to create a nano-sized magnetic sensor with a high sensitivity. However, the nonlinear field dependence of the magnetization and the hysteresis in the magnetization process are serious obstacles for the precise detection of the magnetic field. Therefore, a breakthrough technology based on a different sensing mechanism is required for the innovation of magnetic sensing devices.

As an alternative approach for the sensitive detection of a tiny magnetic field with a high spatial resolution, we are focusing on the ballistic transports in mesoscopic structures. Since the trajectory of the ballistic electron is strongly affected by the external magnetic field, the transport properties of the electrons collimated by patterned nanostructures yields highly sensitive magnetic field response. In fact, the magnetization reversal process of submicron-sized patterned ferromagnets was precisely investigated from ballistic bend resistance measurements using a micro-Hall cross in GaAs/AlGaAs two-dimensional electron gas (2DEG) systems.²⁻⁴ Moreover, a ballistic bend resistance measurement using a 30-nm wide Hall cross was found to show a high spatial resolution of less than 100 nm very recently.⁵ Although the above demonstration using GaAs/AlGaAs 2DEG system is

limited at low temperature, it is not unrealistic in several systems such as graphene to make a device with a channel length less than the mean free path even at room temperature.⁶ Thus, the ballistic transport in 2DEG systems may open an avenue for the development of more functional and higher performance magnetic sensors. Here, we demonstrated that metastable edge domain structures in a ferromagnetic nanowire were sensitively detected by using 2DEG ballistic transports. The study of the edge magnetization is important not only in fundamental physics but also in device applications since the magnetic behavior in tiny magnets strongly depends on the edge condition.⁷⁻¹⁰ Moreover, the ratio of the edge region relatively increases in smaller nanomagnets, which calls for a sensitive magnetic sensor with a high spatial resolution. An anisotropic magneto-resistance (AMR) measurement^{11,12} and a local Hall measurement^{13,14} are well-known methods for electrically detecting a change in the bulk magnetization, however, is difficult to catch up a slight change in the local edge magnetization. In this letter, we show a clear detection of edge magnetic structure in the bend resistance, which indicates that the spatial resolution is much higher than those of other methods. The importance of the ballistic bend signal grows up since the miniaturization of the magnetic sensor is reaching a technological limit nowadays.

A 2DEG cross was fabricated from a GaAs/AlGaAs single-heterojunction wafer. The density and mobility of the 2DEG before processing at 5 K were $4.25 \times 10^{15}/\text{m}^2$ and $76.5 \text{ m}^2/\text{Vs}$, respectively. The depth of the 2DEG plane from the surface is 65 nm. The cross structure $1.2 \mu\text{m} \times 1.2 \mu\text{m}$ was fabricated by means of Ar plasma etching. A scanning electron microscopy (SEM) image of the sample is shown in Fig. 1. The electron mean free path of the 2DEG is $8.2 \mu\text{m}$ at 5 K, which is larger than the size of the cross. A rectangular permalloy (Py) with thickness of 50 nm, width of 900 nm, and length of $10 \mu\text{m}$ is placed on the top of the cross. 4-terminal resistance measurements were carried out using a low-frequency ac technique at 5 K.

We measured a Hall resistance $R_{13,42}$ and a bend resistance $R_{14,23}$ as a function of in-plane magnetic field. We precisely aligned the magnetic field in the 2DEG plane so that

^{a)}Electronic address: mhara@sci.kumamoto-u.ac.jp

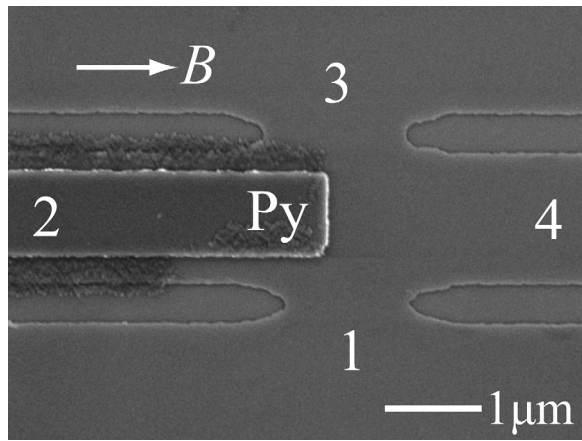


FIG. 1. SEM image of the fabricated device. The 2DEG was etched into a cross structure by Ar plasma etching. The edge of the rectangular Py was placed at the center of the cross. 4-terminal resistance of the 2DEG was measured at 5 K as a function of in-plane magnetic field.

the change in the resistance originates only from a stray magnetic field from the ferromagnet. As shown in Fig. 2(a), the change in the Hall resistance reveals the magnetization reversal of the bulk region. From the local Hall measurement, the reversal field is about ± 10 mT. The change in the bend resistance shown in Fig. 2(b) significantly differs from the Hall resistance and shows a resistance jump at higher fields. These indicate that the bend resistance detects a spatial variation of the stray field from the rectangular Py, which is not apparent in the Hall signal.

In order to analyze the resistance behavior, the magnetization pattern of the rectangular Py was calculated by OOMMF simulator.¹⁵ And then, we estimated the pattern of the stray field normal to the plane of the 2DEG and the total magnetic flux Φ inside the cross. Figure 3(a) shows the magnetic flux as a function of in-plane magnetic field. The magnetic flux dominantly depends on the magnetization of the bulk region. The change in the flux $\Delta\Phi$ with the magnetization reversal of the bulk region is 3.03×10^{-14} Wb. The change in the Hall resistance $\Delta R_{13,42}$ is roughly estimated as the following:^{13,14}

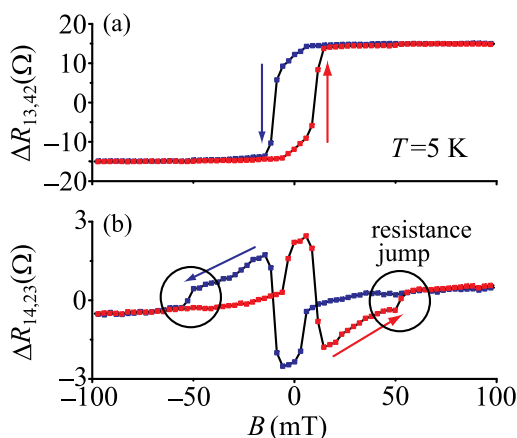


FIG. 2. (a) Hall resistance $R_{13,24}$ as a function of in-plane magnetic field. (b) Bend resistance $R_{14,23}$ as a function of in-plane magnetic field. The offsets are subtracted for clarity.

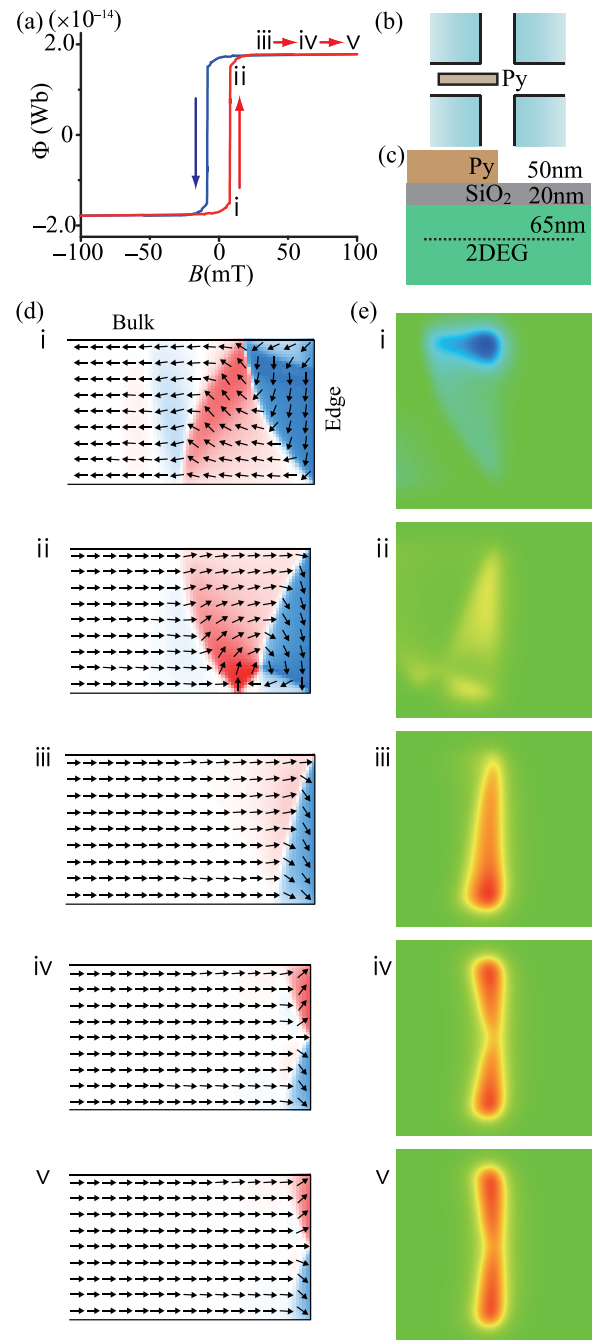


FIG. 3. (a) Estimated magnetic flux Φ in the $1.2 \mu\text{m} \times 1.2 \mu\text{m}$ cross as a function of in-plane magnetic field. (b) and (c) Schematic illustration of the device structure. (d) and (e) Magnetization patterns of the rectangular Py and the stray field profiles in the cross at the sweeping points indicated in (a).

$$\Delta R_{13,42} \simeq \frac{1}{ne} \frac{\Delta\Phi}{S} \sim 30.9 \Omega, \quad (1)$$

which shows a good agreement with the experimental value in Fig. 2(a). Here, S and n are the area of the cross and the electron density of the 2DEG, respectively. The change in the magnetization in this reversal process corresponds to Fig. 3(d) (i \rightarrow ii). In the reversal process, a vortex nucleates at the top or the bottom side near the edge and moves to the other side. Here, the direction of the vortex movement depends on the nucleation site of the vortex determined by the sample asymmetry. At higher fields, the vortex annihilates and then the magnetization only near the edge is not

aligned with the direction of in-plane field as shown in Fig. 3(d)(iii). The tilt direction of the edge magnetization is the same as the direction of the vortex movement. Further increase of the magnetic field leads to a discrete change of the magnetization into a so-called flower state (iii \rightarrow iv).¹⁶ This causes a noncontinuous spatial shift of the stray field while the amplitude of the magnetic flux is almost constant. The change in the magnetic flux due to the transition in the edge region is about 1×10^{-16} Wb. It is quite difficult to detect the transition by a local Hall measurement since the change in the Hall signal is estimated to be about 0.1Ω .

For reproducing the high sensitivity of the bend resistance to the edge magnetic transition, we made a simple simulation based on a semiclassical billiard model.¹⁷ The bend resistance $R_{14,23}$ is described in terms of transmission coefficients between the probes as

$$R_{14,23} = \frac{h}{2e^2} \frac{T_{23}T_{34} - T_{24}T_{31}}{D}, \quad (2)$$

where D is a factor independent of the current/voltage terminal configuration.¹⁸ In the simulation, electrons are injected from each probe like a billiard ball with an angular distribution $P(\alpha) = \cos \alpha/2$. Classical trajectories of electrons are modified by the stray field estimated by the OOMMF simulator. We then calculated transmission probabilities by counting number of the transmitted electrons into each probe.

Figure 4(a) shows the calculated change in the bend resistance $\Delta R_{14,23}$ in the process of the transition between

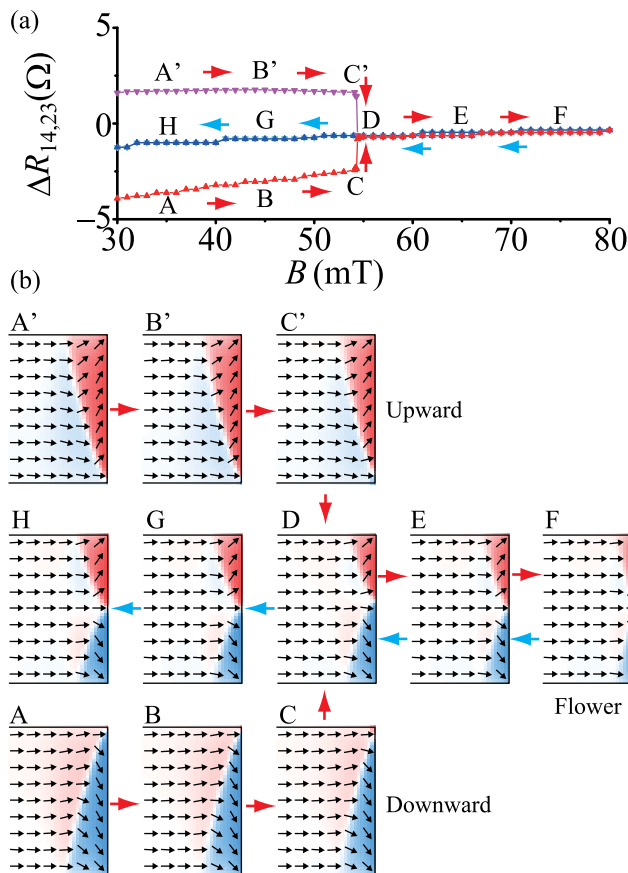


FIG. 4. (a) Calculated change in the bend resistance $\Delta R_{14,23}$ in the process of the transition between meta-stable edge magnetic states. (b) Magnetization patterns near the edge at the sweeping points indicated in (a).

meta-stable edge magnetic states, where the bulk magnetization in the wire is fully aligned in the external field. Corresponding magnetization patterns are shown in Fig. 4(b). Just above the reversal field of the bulk magnetization, there are two possible edge magnetic states (A and A'). The tilt direction of the edge magnetization in the actual sample is determined by an unavoidable sample asymmetry. At higher field, a transition into a more stable flower state occurs in the both paths (C \rightarrow D and C' \rightarrow D). A bend resistance jump due to the edge magnetic transition at $B = 54$ mT is clearly seen in Fig. 4(a). The change in the resistance is about 2Ω which is comparable to the experimental value in Fig. 2(b). Importantly, we can distinguish whether the edge magnetization tilts upward or downward. Comparison with the resistance trace in the experiment reveals that the tilt direction of the edge magnetization before the transition into a flower state was downward in the actual sample, which corresponds to A \rightarrow B \rightarrow C in the simulation. This implies that a vortex nucleated at the top side and then moved to the bottom side in the process of bulk magnetization reversal as shown in Fig. 3(d). If we intentionally make a vortex nucleation site at the bottom, we will observe the other edge magnetization path (A' \rightarrow B' \rightarrow C' in the simulation).

We also calculated the bend resistance behavior for different widths of the rectangular Py to evaluate the spatial resolution for detecting the edge magnetization. Figure 5 shows the calculated change in the bend resistance $\Delta R_{14,23}$ around the transition to a flower state. The transition field increases with decrease of the width of the Py. The shift in the bend resistance between the different edge states is observable even in the narrower cases although the amplitude of the stray field becomes smaller.

Finally, we would like to mention that the present bend resistance measurement is applicable for a multiple-valued magnetic memory.^{19,20} In the present study, the Hall signal reflects the direction of the bulk magnetization (left or right). By contrast, the bend signal is sensitive to the above-mentioned edge magnetic states. Therefore, the combined local Hall/bend measurement enables us to distinguish multiple magnetic states including a slight difference in the edge region. We believe that an approach to a multiple-valued magnetic memory realizes a drastic increase of stored information in magnetic storage devices and the bend resistance

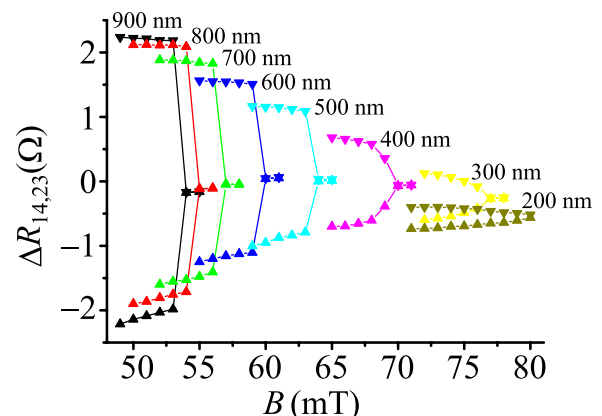


FIG. 5. Calculated change in the bend resistance $\Delta R_{14,23}$ for different widths of the rectangular Py.

measurement plays an important role in reading out the different values.

In summary, we study the behavior of Hall/bend resistance of 2DEG cross in the presence of stray field from the edge of a rectangular Py. The Hall signal is less sensitive to the profile of the stray field and dominantly depends on the magnetization in the bulk region. On the other hand, the bend resistance reveals a magnetic structure in the edge region, which is difficult to detect by the Hall measurement.

We would like to thank the financial support from the Industrial Technology Research Grant Program from NEDO.

¹M. Getzlaff, *Fundamentals of Magnetism* (Springer, Berlin, 2007).

²T. M. Hengstmann, D. Grundler, N. Klockmann, H. Rolf, Ch. Heyn, and D. Heitmann, *IEEE Trans. Magn.* **38**, 2535 (2002).

³M. Hara, J. Shibata, T. Kimura, and Y. Otani, *Appl. Phys. Lett.* **88**, 082501 (2006).

⁴M. Hara and Y. Otani, *J. Appl. Phys.* **101**, 056107 (2007).

⁵A. M. Gilbertson, D. Benstock, M. Fearn, A. Kormányos, S. Ladak, M. T. Emeny, C. J. Lambert, T. Ashley, S. A. Solin, and L. F. Cohen, *Appl. Phys. Lett.* **98**, 062106 (2011).

⁶A. S. Mayorov, R. V. Gorbachev, S. V. Morozov, L. Britnell, R. Jalil, L. A. Ponomarenko, P. Blake, K. S. Novoselov, K. Watanabe, T. Taniguchi, and A. K. Geim, *Nano Lett.* **11**, 2396 (2011).

⁷J. G. Deak and R. H. Koch, *J. Magn. Magn. Mater.* **213**, 25 (2000).

⁸J. P. Park, P. Eames, D. M. Engbreton, J. Berezovsky, and P. A. Crowell, *Phys. Rev. Lett.* **89**, 277201 (2002).

⁹R. D. McMichael and B. B. Maranville, *Phys. Rev. B* **74**, 024424 (2006).

¹⁰F. Guo, L. M. Belova, and R. D. McMichael, *Phys. Rev. Lett.* **110**, 017601 (2013).

¹¹B. Hausmannsa, T. P. Kromea, G. Dumpicha, E. F. Wassermann, D. Hinzkeb, U. Nowakb, and K. D. Usadelb, *J. Magn. Magn. Mater.* **240**, 297 (2002).

¹²M. Bolte, M. Steiner, C. Pels, M. Barthelmeß, J. Kruse, U. Merkt, G. Meier, M. Holz, and D. Pfannkuche, *Phys. Rev. B* **72**, 224436 (2005).

¹³M. Johnson, B. R. Bennett, M. J. Yang, M. M. Miller, and B. V. Shanabrook, *Appl. Phys. Lett.* **71**, 974 (1997).

¹⁴A. K. Geim, S. V. Dubonos, J. G. S. Lok, I. V. Grigorieva, J. C. Maan, L. Theil Hansen, and P. E. Lindelof, *Appl. Phys. Lett.* **71**, 2379 (1997).

¹⁵M. Donahue and D. Porter, Interagency Report No. NISTIR 6376, National Institute of Standards and Technology, Gaithersburg, MD, 1999.

¹⁶D. Goll, G. Schütz, and H. Kronmüller, *Phys. Rev. B* **67**, 094414 (2003).

¹⁷C. W. J. Beenakker and H. van Houten, *Phys. Rev. Lett.* **63**, 1857 (1989).

¹⁸M. Büttiker, *Phys. Rev. Lett.* **57**, 1761 (1986).

¹⁹T. Kimura and M. Hara, *Appl. Phys. Lett.* **97**, 182501 (2010).

²⁰S. Khym, T. Yoo, H. Lee, S. Lee, S. Lee, X. Liu, J. K. Furdyna, D. U. Lee, and E. K. Kim, *Appl. Phys. Express* **5**, 093004 (2012).